Improving Predictions of Snow Resources Using Midlatitude SSTs with Convergent Cross Mapping

H Kim[1], D Fastovich[1], T Bhattacharya[1], and S E Tuttle[1]

[1]Department of Earth and Environmental Sciences, Syracuse University, Syracuse, NY, USA

E-mail: hkim139@syr.edu

February 2025

Abstract. Effective water resource management in the western United States (WUS) is possible only with accurate monitoring and forecasting of seasonal snowpacks. Seasonal snowpack, a major water source for the WUS, is declining due to anthropogenic climate change. Overprinted on this trend is year-to-year variance in snowpack extent and mass due to influences from teleconnections related to the El Niño Southern Oscillation (ENSO) and the Pacific Decadal Oscillation (PDO). Recently in the 2015 and 2016 winters, extreme droughts in the coastal WUS, mainly the Pacific Northwest (PNW) states of Washington and Oregon were linked with anomalously warm sea surface temperatures (SST) in northeastern Pacific Ocean. Here, we use convergent cross maps (CCMs) to analyze time series of SSTs and snow water equivalent (SWE) in the PNW. For some ecoregions, we show that extratropical SSTs may have a stronger influence on snowfall and snow accumulation in the PNW compared to tropical indices of climatic variability. Cold (warm) SSTs in the northeast Pacific lead to high (low) snow years. CCMs also performed better in recreating SWE anomalies compared to linear regressions with lagged predictor variables. Accounting for the influence of SSTs may help water resource managers to better predict and prepare for extreme snow events in the future.

Keywords: Snow, Pacific Northwest, Convergent Cross Maps

Submitted to: *Environ. Res. Climate*

1. Introduction

Snow is a major water source globally and in the western United States (WUS). Snow in montane and alpine regions act as natural water towers and feeds the water needs of over 60 million people [1, 2]. The resulting snowmelt accounts for over 70% of the total runoff in the mountainous regions of the WUS (e.g., Sierra Nevada, Cascades, and Rockies) [3]. Anthropogenic climate change has reduced both the extent and duration of the seasonal snowpack [4]. Increased winter temperature has decreased

the percent of winter precipitation falling as snow and has led to earlier peak snowmelt [4, 5], producing a mismatch between water demand and supply. Compounding these challenges, snowpack deficits or snow droughts have increased in frequency in the past 30 years in the Pacific Northwest (PNW) [6].

Predicting the amount of snow and timing of snowmelt is critical for effective water resource management. Snow has a wide variety of uses that ranges from recreation to climate regulation [7]. The water from snowmelt provides water for ecosystems, urban centers, agricultural production, and hydroelectric power generation [3, 8]. Snow forecasting is also needed for managing growing natural hazards. Damages from some major floods resulted partly from underpredictions of snow resources [9], and the frequency of rain-on-snow events, where flooding occurs due to melting of snow from warmer rain events, is expected to increase as the climate continues to warm [10, 11]. Despite the need for accurate snowpack monitoring, current estimates of the water stored as seasonal snow, or snow water equivalent (SWE), is highly uncertain [12]. Seasonal snow is spatially variable at multiple scales and there are current limitations to SWE data collection and satellite retrievals [12].

The challenges of snow monitoring are compounded by the year-to-year variability in seasonal snowpacks. Atmospheric adjustments from the teleconnections of interannual (e.g., El Niño Southern Oscillation (ENSO)) and interdecadal (e.g., Pacific Decadal Oscillation (PDO)) climatic variability contribute to seasonal snowpack variability [13]. Remote teleconnections amplify wet and dry years, leading to uncertainties in yearly precipitation and snowpack levels. In the past decade, snowpack in California varied from extreme highs in 2023 [14] to extreme lows between 2011 to 2016. Similar droughts also affected other WUS states including the PNW states of Washington and Oregon, with record low snowpack levels in the 2014 and 2015 winters [15]. Although the interannual and interdecadal variability in seasonal snowpack is well-documented [13, 14, 16–18], it is difficult to pinpoint the causal drivers of this variability since several modes of climate variability are all interconnected.

Recent events have shown that sea surface temperatures (SSTs) may also play a role in amplifying wet and dry years. Anomalously warm "blobs" of SSTs across the northeast Pacific contributed to wide-scale drought across the WUS. Seager *et al* (2015) noted that the 2011-2014 historical California drought was first onset by a La Niña event but increases in SST off of the coast of California exacerbated drought-like conditions into a multi-year drought [19]. The warming of SST off the coastal WUS caused a ridge pattern (anomalously high pressures) to build, which inhibited moisture fluxes and precipitation formation [15, 19–21]. These studies suggests that SSTs may play a large role in affecting winter precipitation patterns, in addition to the modes of climatic variability. To what extent and where has not been fully examined.

Here, we use Convergent Cross Mapping (CCM) [22], a causal inference method, to examine whether SSTs in the eastern Pacific Ocean are causally related to snowpack levels in PNW mountain ranges. We identify regions where extratropical SSTs are affecting WUS snowpack levels through atmospheric adjustments and teleconnections.

We also show whether CCMs can make better reconstructions of PNW SWE using the prior SST dynamics of the northeast Pacific Ocean.

In the next sections, we describe the data used in this analysis and detail the CCM algorithm (section 2). The CCM results are presented and discussed in section 3.

2. Data and Methods

2.1. Snow Data

The target variable of our analysis is SWE in the WUS and Canada from the dataset compiled by Musselman (2021) [23]. Western North America (WUS and Canada) has one of the most extensive networks of automated snow observations in the world, with low biases compared to co-located ground observations [24, 25]. SWE at these stations are measured daily through a snow pillow that weighs the amount of snow fallen on the ground with a pressure transducer and converts the weight to its water equivalent [25, 26]. Quality controlled daily SWE measurements are available from Oct. 1, 1960 until September 1, 2019 (a period of 59 years) from snow stations managed by various agencies including the Natural Resources Conservation Service (NRCS), the California Department of Water Resources (DWR), Alberta Environment (AB), the British Columbia Ministry of Environment (BC), and the Yukon Government Water Resources Branch (YK) [25].

Snow in the WUS is not monolithic, its accumulation and melt dynamics can vary according to different snow and climate regimes [27]. Snow can also vary with ocean-atmosphere teleconnections such as ENSO [13, 28]. As a result, we subset the SWE data using the Level III Ecoregions in the WUS and Canada defined by the United States Environmental Protection Agency [29]. For this study, we limited our analysis to four PNW ecoregions: the North Cascades, the Cascades, the Eastern Cascades Slopes and Foothills, and the Columbia Mountains/Northern Rockies. Table 1 summarizes the PNW ecoregions used in this analysis including when the first snow station measurements were made and how many snow stations are located within each ecoregion. Of the 1,065 snow stations in the dataset, 182 stations are located within our ecoregions of focus. All stations that were located within the boundaries of an ecoregion were grouped together, and averaged into a single SWE time series. To do this, daily SWE measurements for each snow station were aggregated to a monthly timestep. Then, the climatological monthly means were removed to obtain monthly SWE anomalies. Each snow station may experience different snowpack magnitude and timing due to site-specific conditions (e.g., altitude, aspect). Therefore, we normalized the SWE anomalies by the climatological monthly standard deviations across all years to reduce the potential bias during averaging. The number and location of snow monitoring stations was variable throughout the time range of our data (see table 1 and table S1). For each ecoregion, we reduced all data into a single SWE anomaly time series by taking the average of all stations. The results of the other 11 WUS ecoregions are included in

Table 1. Description statistics of Pacific Northwest ecoregions used in this analysis including the number of stations within the ecoregion, the start date of measurements, the length of the time series in number of months, and which agency manages the stations within the ecoregion.

Ecoregion	Num. of Stations	Start Date	Length	Sources
Columbia Mountains/Northern Rockies	59	1 Oct. 1966	636	BC, NRCS
North Cascades	32	1 Oct. 1973	531	BC, NRCS
Cascades	66	1 Oct. 1978	492	DWR, NRCS
Eastern Cascades Slopes and Foothills	25	1 Oct. 1978	478	DWR, NRCS

the Supplementary material (Figures S1 to S3).

2.2. SST Data

For the SST data, we used National Oceanic and Atmospheric Administrations' (NOAA) Extended Reconstructed Sea Surface Temperature, version 5 (ERSST) with a spatial resolution of 2° x 2° [30]. The current version of the ERSST uses data from the International Comprehensive Ocean-Atmosphere Dataset Release 3.0, Argo floats, and Hadley Centre Ice-SST version 2. We bounded the ERSST into distinct regions within Pacific Basin (20°S to 60°N and 180° to 80°W) and temporally between 1960 to 2019, to align with SWE measurements. SST anomalies were calculated by removing the climatological monthly means for each grid cell.

2.3. CCM

We use convergent cross mapping (CCM) to quantify the causal relationship between time series of SST and SWE anomalies. CCM infers causality of two variables, X and Y, within a nonlinear dynamical system by evaluating the degree to which two variables behave consistently when revisiting similar states [22, 31]. Specifically, CCM tests whether X causes Y if the causal variable, X, imprints an information signature on the affected variable, Y [29]. We find these imprints by taking cross-maps of X from the shadow manifold of Y, M_y, or the set of all lagged or historical values of Y. The number of lags used to construct the shadow manifold is E, the embedded dimension. For each time step, $E + 1$ nearest neighbors are identified in M_y using the Euclidean distances of Y within a subset length of the shadow manifold that constrains where nearest neighbors can be identified [31]. The time indices of these nearest neighbors are used to map points in X. The forecast variable X^* is computed by averaging the nearest neighbors in X by the Euclidean distances in M_y. The strength of causality or CCM cross-map skill (shortened to CCM skill) is the Pearson's correlation between the observed X and the forecasted X^*. These steps are repeated using an increasingly larger fraction of time series length or library size. We conclude X causes Y with a high CCM skill that converges with increasing library size. CCM can detect non-linear state

dependent relationships and also accounts for directional couplings of variables (e.g., X may causally influence Y but not vice-versa) [32]. CCM has been used in a wide variety of studies to infer the causality between anchovy populations and North Pacific SSTs [22], soil moisture and precipitation [33], atmospheric blocking events [34], and groundwater and streamflow [31]. We used the freely available python package pyEDM (https://github.com/SugiharaLab/pyEDM), a python version of the rEDM package [35], to run the CCM analysis.

We performed CCM analyses for each grid cell of our SST data against a time series of SWE anomalies for each PNW ecoregion of focus. Before the CCM analyses, we calculated SST and SWE anomalies (see sections 2.1 and 2.2 for details) and the optimal Embedding Dimension, E. We used the built-in function EmbedDimension() in pyEDM to obtain the maximum E that returns the highest prediction skill between 1 and 10. Figure 1 summarizes the process described above for performing a CCM analysis. A time series of normalized SST anomalies (figure 1(c)) for a grid cell (black box, figure 1(a)) are compared against a time series of SWE anomalies (figure 1(b)). The Cascades ecoregion is highlighted in orange on figure 1(a). The CCM analysis was conducted for three different lag periods: 1 month, 3 months, and 6 months, for each of the four PNW ecoregions to test for seasonal or sub-seasonal relationships. While CCMs can identify bidirectional couplings, this analysis focuses on how SSTs are driving SWE, since we expect SSTs drive large-scale atmospheric conditions that influence SWE.

For this analysis, CCM skills are statistically significant if it exceeded the skill of a CCM analysis that used surrogate data, thus showing a causal relationship between SSTs and SWE. We used surrogate data that retained the seasonal trends but incorporated randomness that erased any sub-seasonal causal links between SSTs and SWE, following a methodology similar to Cenci and Saavedra (2019) [36]. We generated surrogate data of 200 randomly sampled SST grids within the eastern Pacific Ocean for six WUS ecoregions (three in the PNW and three other ecoregions outside the PNW). We used the SurrogateData() function in the pyEDM package using the seasonal method and ran CCM analyses to establish our baseline. The upper limits of these analysis at 95% confidence showed CCM skills at least 0.14, 0.21, and 0.25 for lags 1, 3, and 6, respectively, would be statistically significant. Any CCM skill values for SST anomlaies above 0.3 is considered to be statistically significant.

3. Results and Discussion

Figure 2 shows the CCM skill for each grid cell of the SST data against the PNW coastal ecoregions for a lag of one month, three months, and six months, respectively. SSTs near the northeast (NE) Pacific have a strong causal relationship with SWE values with particularly strong relationships in the North Cascades and the Cascades ecoregions (figure 2(a)-(c) and 2(d)-(f), respectively) across all lags. We define an area of interest in the NE Pacific Ocean (hereafter the "NE Pacific") between 40°N to 50°N and 140°W to 130°W (black boxes in figure 2), southeast of the Gulf of Alaska

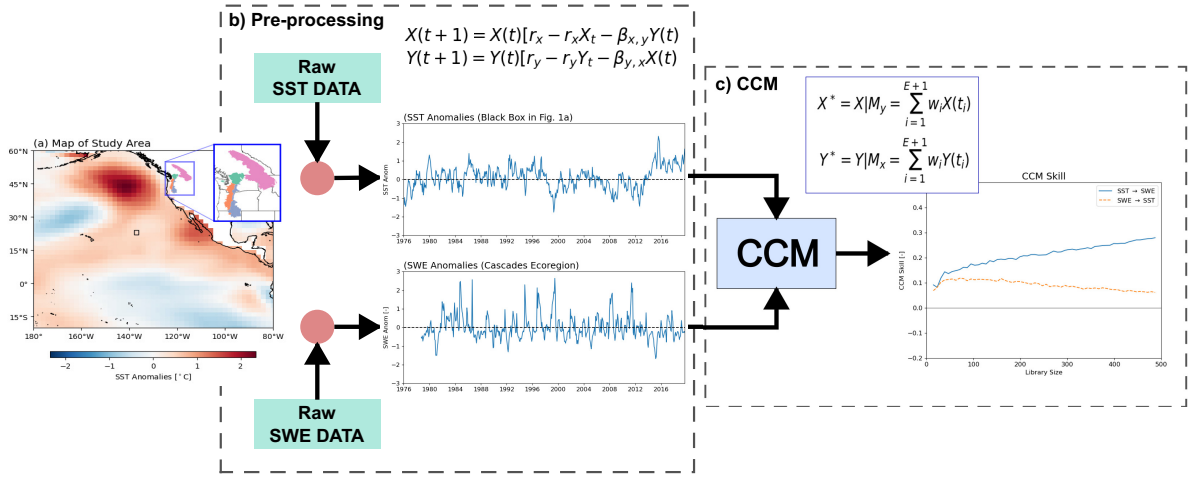

Figure 1. (a) Map of the study area of sea surface temperature (SST) anomalies of the eastern Pacific Ocean (20°S to 60°N and 180° to 80°W) on 3 March 2014 and the 4 EPA Level III ecoregions on the Pacific Northwest: Cascades (orange), North Cascades (green), Eastern Cascades Slopes and Foothills (blue), and Columbia Mountains/Northern Rockies (pink). A flowchart of our analysis is shown. (b) The raw SST and SWE data are processed and transformed. The raw data is aggregated and normalized following the steps outlined in sections 2.1 and 2.2 to calculate a SWE and SST anomalies, respectively. (c) We conducted a CCM analysis between the SST and SWE anomalies. CCMs compares the observed X to the forecasted X^* which is given as an estimate of X given the nearest neighbor historical values of Y (or the shadow manifold, M_y). The CCM analysis can be generalized for any sample nonlinear system where X is explicitly defined to influence Y by a factor of β and constants r_x, r_y controls how chaotic the system is [22]. The CCM skill is the Pearson's correlation between X and X^* for increasing fractions of the library size. While CCMs can also interpret directionality of causality, we are only focused on how SSTs affect SWE (blue line in box c).

where the Pacific Current bifurcates into the Alaska and California Currents. For the Eastern Cascades Slopes and Foothills (hereafter Eastern Cascades) and the Columbia Mountains/Northern Rockies (hereafter Columbia Mountains) ecoregions, we observe weaker causal relationships between SSTs in the NE Pacific and SWE compared to the Cascades and North Cascades. The weakest relationship is found with the Columbia Mountains, which does not meet our threshold of statistical significance at all lags. Increasing the lag from one to three and six, increases the CCM skill to where SSTs are causally linked with Eastern Cascades SWE.

To assess whether the predictability of snow resources can be improved by incorporating extratropical SSTs into forecasts, we performed additional CCMs using NE Pacific SST anomalies against PNW SWE. NE Pacific SSTs were averaged and anomalies were calculated as described in section 2.2. Figure 3 shows the CCM skill of how SWE is influenced by NE Pacific SSTs compared against ENSO and PDO indices. We used monthly Niño3.4 and PDO indices from NOAA's Climate Prediction Center and Physical Sciences Laboratory, respectively (see section S2 in Supplementary Materials).

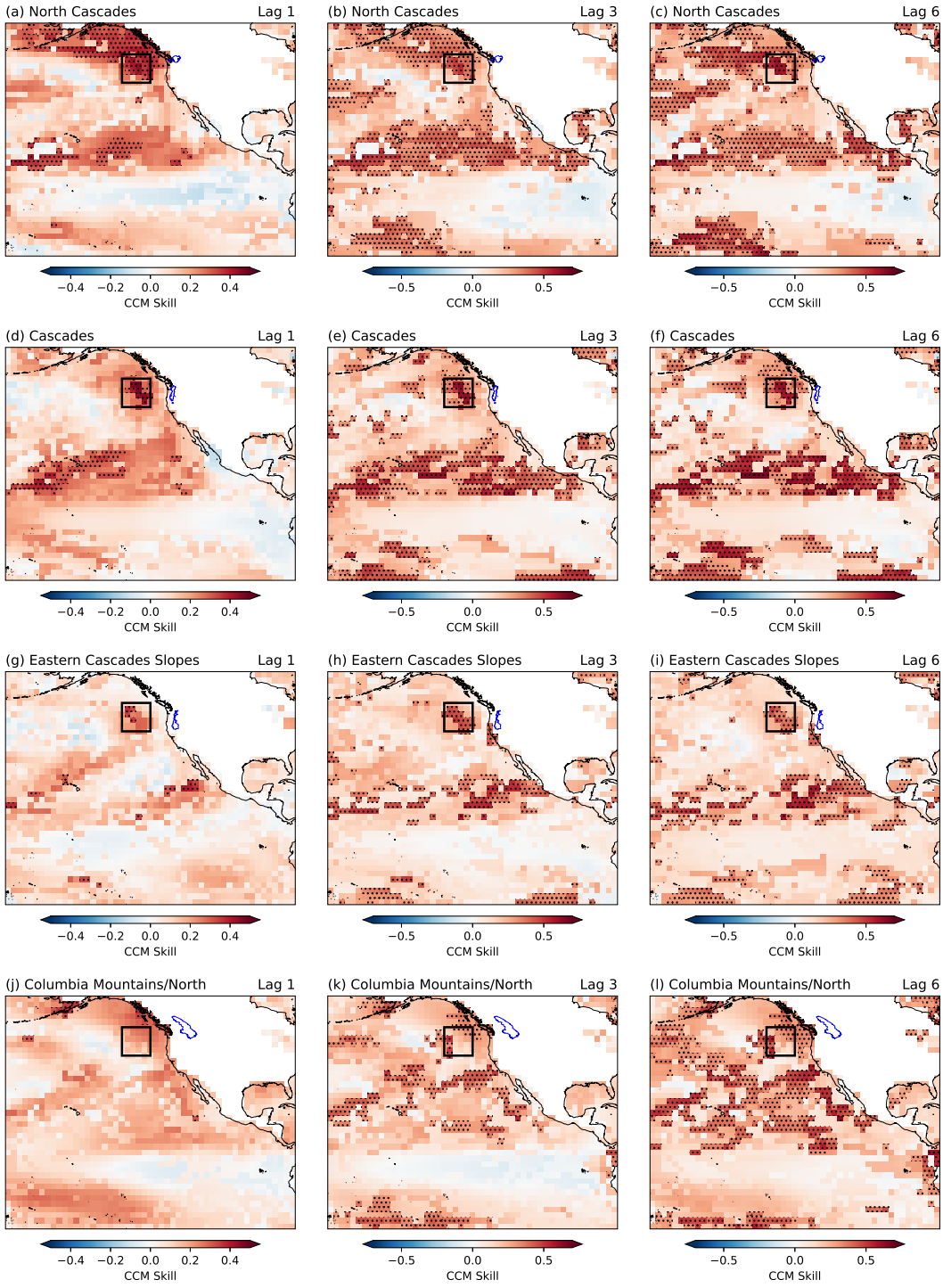

Figure 2. Cross-mapped skill of the SST influence on SWE for each grid cell in the research domain for the (a)-(c) North Cascades, (d)-(f) Cascades, (g)-(i) Eastern Cascades Slopes and Foothills, and (j)-(l) Columbia Mountains/Northern Rockies ecoregions with lags of 1 month (left column), 3 months (center column) and 6 months (right column). All statistically signficant grid cells with CCM skills greater than 0.3 are stippled. The boundary of the NE Pacific is shown (black box on (a)-(l)).

For all of the PNW ecoregions except for the Columbia Mountains, NE Pacific SSTs had greater CCM skills compared to either ENSO or PDO across all lags. In the North Cascades, Eastern Cascades, and the Columbia Mountains, PDO tended to have a stronger causal relationship on SWE compared to ENSO. Figure 3 shows that our index focused on extratropical SST variability has a larger influence snowpack levels than tropical/subtropical indices such as ENSO and PDO. Other research has noted the sensitivity of Cascades snowpack to North Pacific sea level pressure and circulation patterns from annual to interdecadal time scales [37].

Figures 4 to 6 compare the observed SWE anomalies (black dotted lines) with the CCMs predictions based on NE Pacific SSTs (blue lines) for three out of the four PNW ecoregions (Cascades, North Cascades, and Columbia Mountains). For the Cascades ecoregion on figure 4, we observe Pearson's correlation of 0.38 and 0.36 between the observed SWE anomalies and the CCM reconstructions from lags 1 and 6, respectively. Correlations were slightly lower at lag 3 for the Cascades with a value of 0.33. For the North Cascades ecoregion (figure 5), we observe that CCMs can better predict SWE as we increase the lag from 1 month to 6 months (0.33 to 0.60). The Columbia Mountains ecoregions (figure 6) have the worst performance of the 3 coastal ecoregions, with a maximum correlation metric 0.31 at lag 6. However, CCM reconstructions are more correlated with observations in the Columbia Mountains as the lag increases from 1 month to 3 months to 6 months (0.21 to 0.30 to 0.31, respectively).

To show CCMs provide better predictions than commonly used methods, we also generated SWE predictions from lagged linear regression models (orange lines on figures 4 to 6). The lagged linear regression used NE Pacific SSTs to predict SWE in the future one, three, or six months ahead, with observed SST as the dependent variable. For example, a lag 3 linear regression predicts SWE 3 months in the future from current SST values. In all three of the ecoregions compared, the Pearson's correlations for the linear regressions decreases as the lag increased when compared to the observations. In the Cascades (figure 4), the correlation was 0.41 at lag 1 and dropped to 0.29 at lag 6. Similarly to the Cascades, the linear regression for the North Cascades (figure 5) and the Columbia Mountains (figure 6) follows a similar pattern. Correlations decreases from 0.39 to 0.23 in the North Cascades and decreases from 0.323 to 0.199 in the Columbia Mountains/North Rockies.

As lags increase, the linear regression time series of SWE also appears to be smoothed compared to the CCM predictions in figures 4 to 6. Figure 7 shows how the lagged linear regression SWE predictions compare against both SWE observations and CCM predictions in the North Cascades for 4 recent high and low snow years. Similar graphs for the other ecoregions are provided in the supplemental materials. A perfect prediction of SWE anomalies would fall on the 1:1 line (black dashed line) on figure 7(a). The slope of the predictions from the linear regressions were 0.04 compared to the CCM slope of 0.48. Additionally, the slope of the linear regression is not statistically different from 0 at a significant level of 0.05%. This is further shown comparing the mean absolute error (MAE) of predicted SWE anomalies. Figure 7(b) shows the MAE for the linear

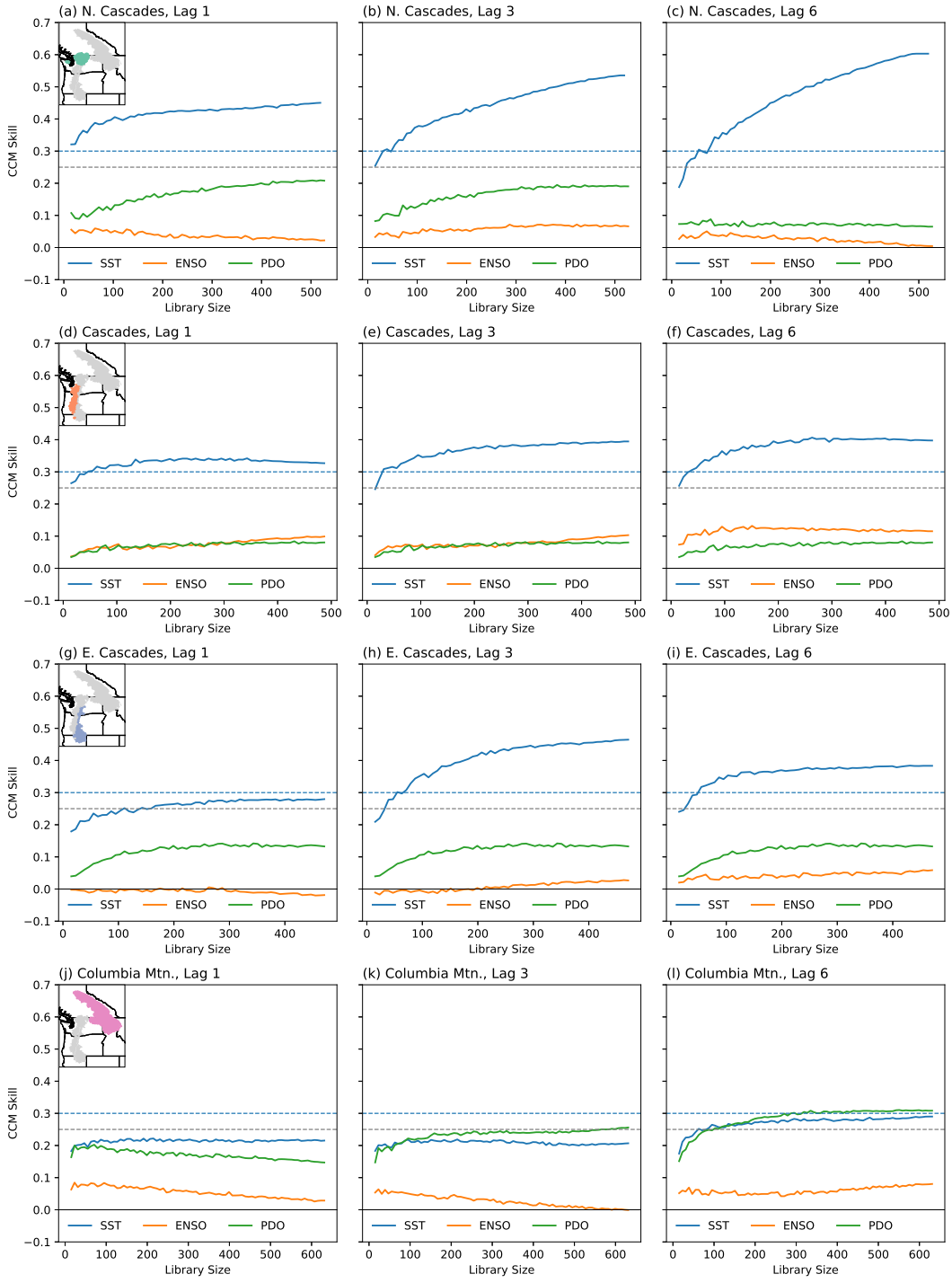

Figure 3. Cross-mapped skill of the NE Pacific SST (blue line), ENSO (orange lines), and PDO (green line) influence on SWE in the (a)-(c) North Cascades, (d)-(f) Cascades, (g)-(i) Eastern Cascades Slopes and Foothills, and (j)-(l) Columbia Mountains/Northern Rockies ecoregions with lags of 1 month (left column), 3 months (center column) and 6 months (right column) for each grid cell for SST anomalies. The dashed blue line is the limit to which the SST CCM analysis are statistically significant. The dashed grey line is the limit of the ENSO and PDO CCM analyses are statistically significant.

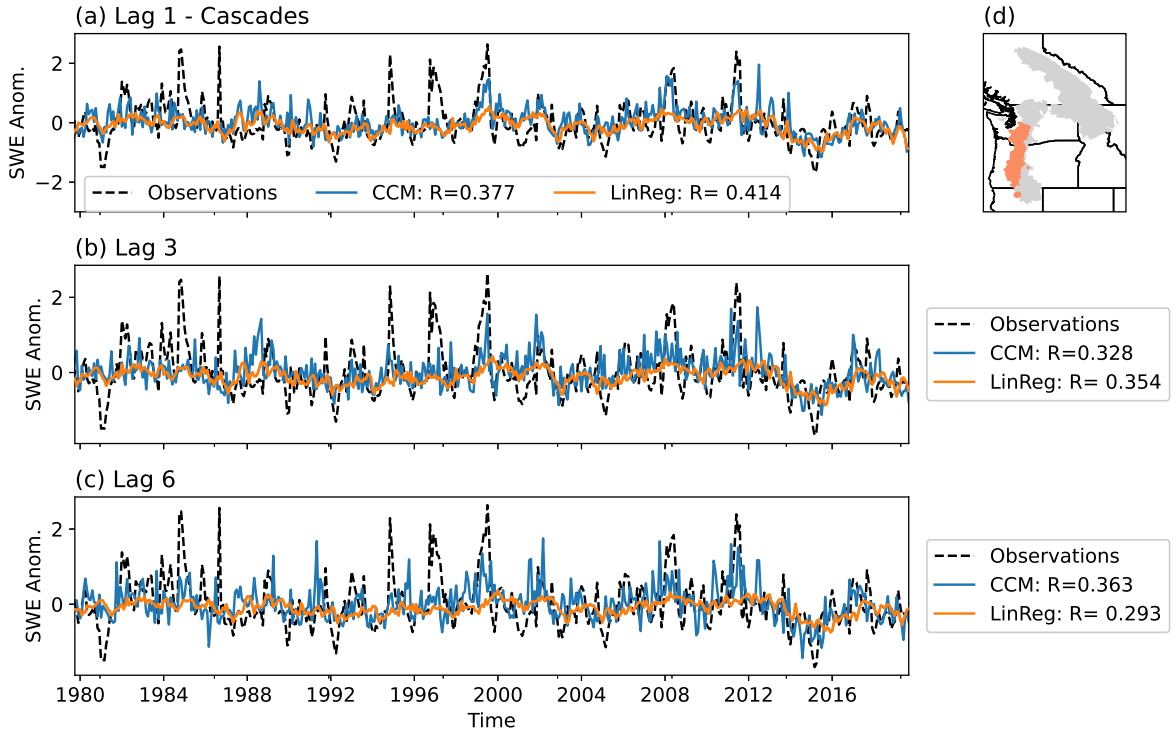

Figure 4. Comparisons between SWE anomalies from observations (grey dotted line) against CCM (blue line) and a lagged linear correlation (orange line) for lags of (a) 1 month, (b) 3 months, and (c) 6 months for the Cascades ecoregion. The CCM and linear regressions were calculated using SST anomalies from the NE Pacific. (d) A map of the ecoregion is provided for context.

regression predictions are larger for all water years except for one, showing the linear regressions are not predicting SWE anomalies as well as the CCMs, especially at a lag of 6 months. A linear regression will simply predict the state of a dependent variable (i.e., SWE) from the state of an independent variable (i.e., SSTs). The nature of the CCM analysis comparing similar dynamical histories through the simplex projection [38, 39] provides better predictability at higher lags, accounting for SST changes that are linked with different climatic modes of variability.

The CCM results further show that snowpack levels in the PNW are sensitive to the different modes of climatic variability. For example, CCM reconstructions in the Cascades (figure 4) improve after 1999, indicated by the Pearson's correlations (0.15 and 0.47 from the lag 1 results, for pre-1999 and post-1999, respectively). These patterns were also found in the lags 3 and 6 CCMs for the Cascades. We hypothesize this change in predictability is due to a shift in the PDO around 1998/1999 (see figure S5(b)). This possibly suggests the atmospheric responses are amplified depending on the temperature difference between the eastern Pacific PDO pattern and our NE Pacific SST. Previous research has shown in the Cascades Mountains snow decreased by 48% between 1950 to 1997 and increased by 19% from 1976 to 2007 [37]. This phenomena was only observed in the Cascades ecoregion in this analysis.

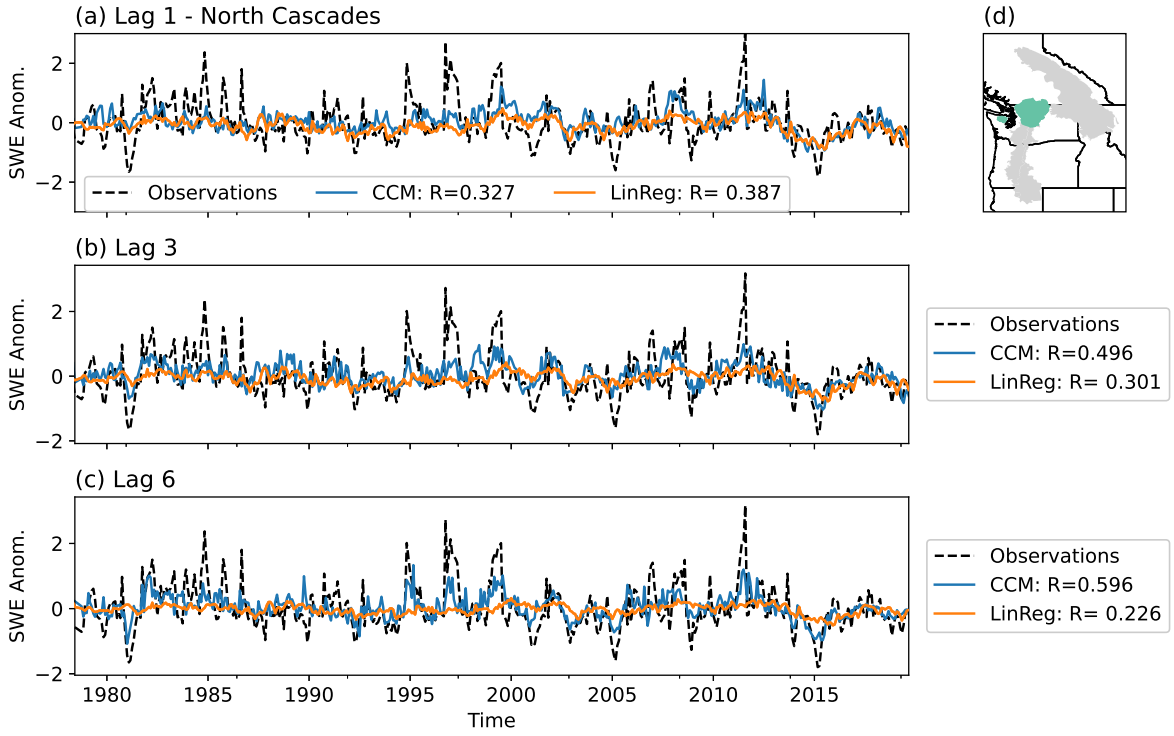

Figure 5. Same as figure 4 but for the North Cascades ecoregion.

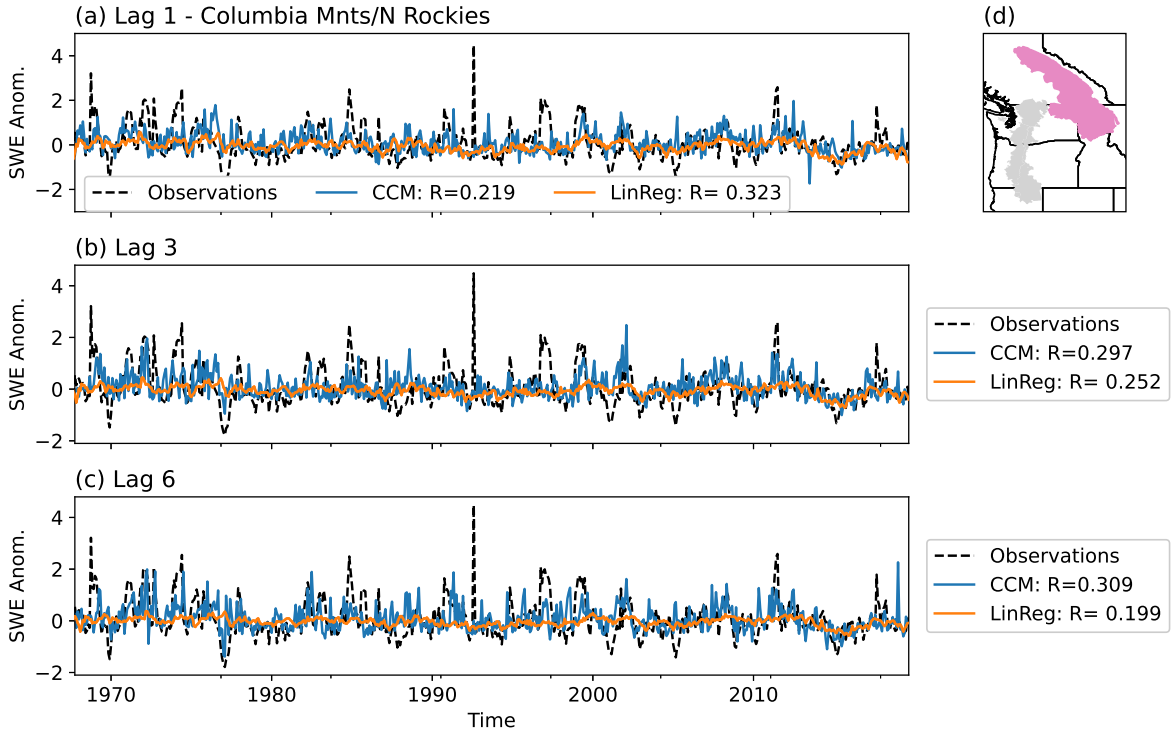

Figure 6. Same as figure 4 but for the Columbia Mountains/Northern Rockies ecoregion.

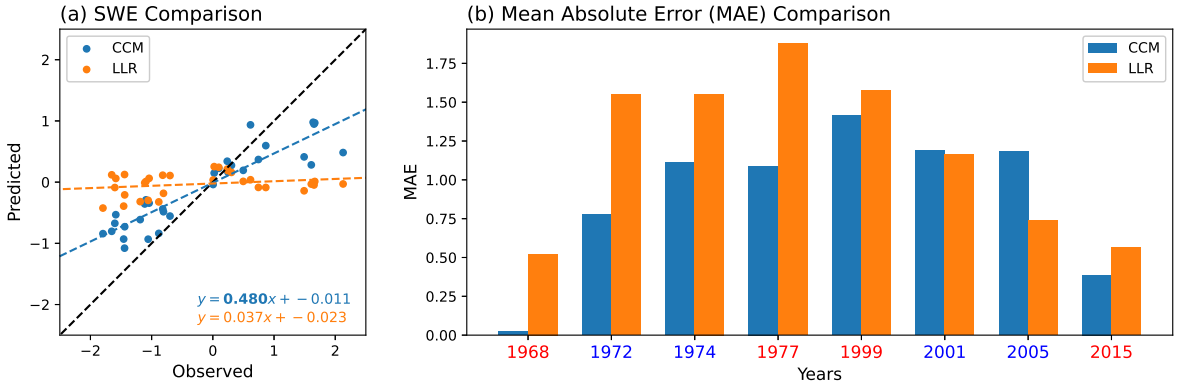

Figure 7. (a) Comparisons of predicted vs observed SWE anomalies for the 4 highest and 4 lowest snow years for the North Cascades ecoregion. Lag 6 linear regression (LLR, orange dots) failed to predict SWE anomalies compared to the lag 6 CCMs (blue dots), especially compared to the 1:1 line (dashed black line). (b) Comparisons of the mean absolute error (MAE) of the predicted SWE anomaly compared to the observed. Larger errors denote worse predictions for the highest (blue) and lowest (red) snow years. In general, linear regressions did worse in predicting the SWE anomaly compared to the CCM.

While we demonstrate that CCMs can predict SWE using SST dynamics, CCMs do not reveal the direction of causality between SST dynamics and SWE. To understand how SSTs affect SWE in their respective PNW ecoregions, we plotted composites of the average NE Pacific SST anomalies during all high and low snow years for the Cascades, North Cascades, and Columbia Mountains (figure 8). Our definitions of high and low snow years are listed in section S1 of the supplementary materials. Figure 8 shows that low snow years are generally related to positive SST anomalies (warmer SSTs) in the NE Pacific. High snow years are related to negative SST anomalies (colder SSTs) in the NE Pacific. There is more variability in the high snow years compared to the low snow years, but most of the variability occurs at or after the peak SWE and into the following summer. The low snow years were generally the same for the three ecoregions shown.

To assess prior hypotheses that atmospheric adjustments due to SSTs can affect snowfall in the PNW, we plotted the monthly mean sea level pressure (SLP) for high and low snow years using the European Centre for Medium-Range Weather Forecasts (ECMWF) Reanalysis v5 (ERA5) for the entire northern Pacific basin (figure 9). Our reference for the lags is 1 April, near to the mean annual date of maximum SWE. For the high and low snow years, we observe differing Rossby wave trains that affect precipitation along the PNW. The mean SLP configuration for a high (low) snow year has high (low) pressures over the Central North Pacific Ocean, especially during lag 3 (figure 9(b)) and lag 1 (figure 9(c)). Additionally, these Rossby wave trains resemble atmospheric pressure configurations for La Niña in high snow years and El Niño in low snow years. We also observe some ridging or a build-up of high pressures either near or above the PNW ecoregions used in this study. The anomalous circulations created by

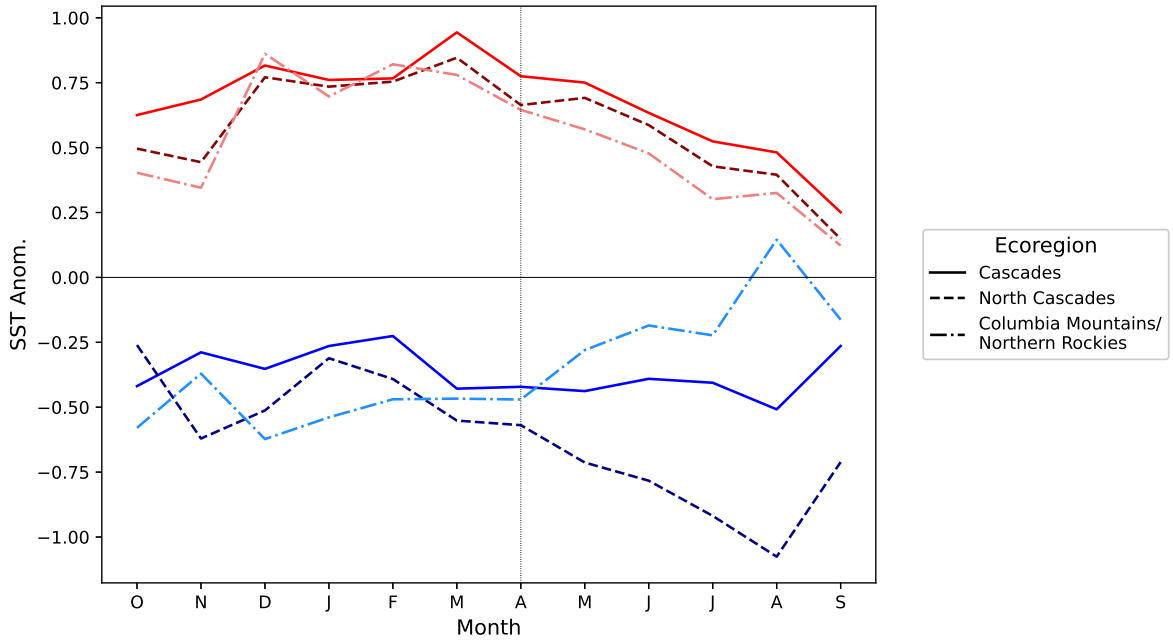

Figure 8. Average SST anomaly composites for all high snow years (blue lines) and all low snow years (red lines) for the Cascades (solid lines), North Cascades (dashed lines), and Columbia Mountains/Northern Rockies (chained lines) ecoregion, averaged over the NE Pacific. High (low) snow years are associated with negative (positive) SST anomalies.

the high pressure centers during high snow years would direct storms towards the PNW ecoregions, while low pressure in low snow years would direct storms away. During high snow years, the low pressure center would bring onshore flow or westerly winds towards the PNW ecoregions. The pressure centers during low snow years bring offshore flow or easterly winds, which would be dryer and inhibit precipitation formation. Our results are similarly supported in the literature, where temperature and onshore flow largely controlled the precipitation and snowpack levels of the Cascades Mountains [37].

Figure 10 shows a similar plot for SSTs during high and low snow years at lags 1, 3, and 6 before April. For both high and low snow years, we observe strong, seasonally persistent SST signals in the NE Pacific. We contrast these to SST anomalies near the equator, which show changes in the central Pacific consistent with shifts in ENSO phase. For instance, high snow years show cool La Niña-like anomalies in the Central Pacific, while low snow years show slightly warm El Niño-like anomalies. This suggests that the dynamics responsible for snow variability are not unrelated to ENSO, but that extratropical SSTs offer an improved ability to predict high/low snow years over and above the predictability provided by ENSO indices.

The strong persistent nature of SSTs in the NE Pacific, especially in low snow years, is likely the cause of the higher CCM skill. While the ENSO will largely set up atmospheric patterns that are preferential to snowfall, extratropical teleconnections and the atmospheric adjustments from warm SSTs can have an amplifying effect on

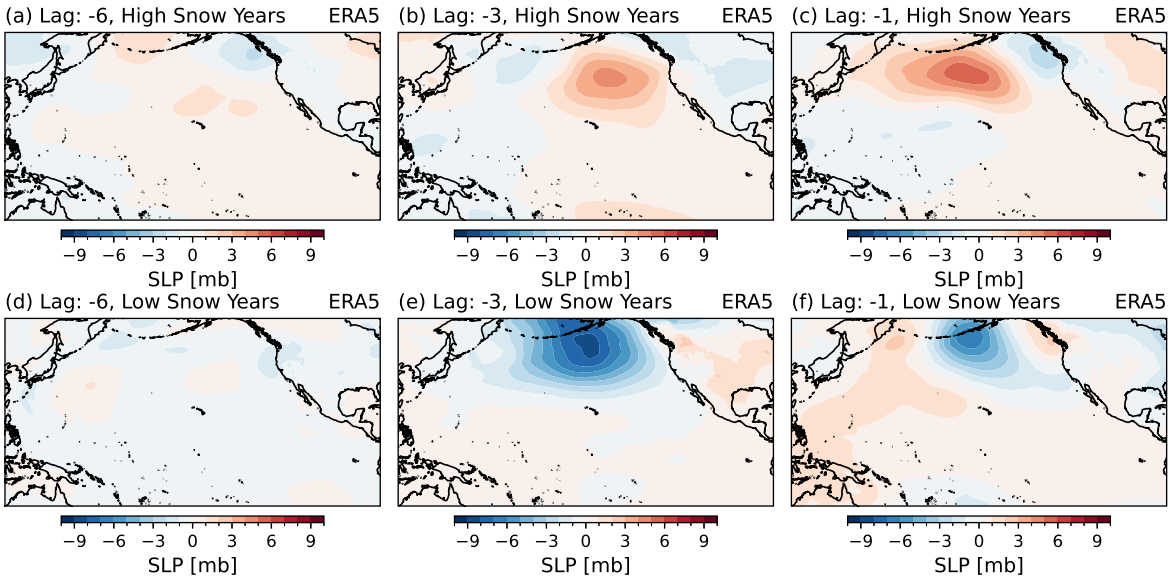

Figure 9. Mean sea level pressure anomalies at lags of (a) 6 months, (b) 3 months, and (c) 1 month prior to April, when maximum SWE is generally achieved, for all high snow years in the Cascades ecoregion. Mean sea level pressure anomalies are plotted for lags of (d) 6 months, (e) 3 months, and (f) 1 month for all low snow years for the Cascades ecoregion.

these ENSO teleconnections [40]. Other studies have also noted the interplays of the North Pacific Oscillation (NPO) with wind-evaporation-SST feedbacks [41–43]. Notably, Baxter and Nigam (2015) noted that North American winter climate anomalies in 2013/14 were due to the NPO-West Pacific teleconnection and do not need to originate in the tropics [43]. This study focused on the entire United States, but are generally aligned with our findings in the PNW. Other studies have mentioned that the North Pacific Meridional Mode from the spring can lead ENSO signals in the following winter [44, 45].

Many studies agree that Pacific SST anomalies can modify the intensity and position of the midlatitude storm tracks; several studies propose the coupling between SST anomalies in the North Pacific and changing baroclinicity [46, 47]. Gan *et al* (2013) showed that storm tracks were coupled with SSTs on seasonal timescales, with warm SST anomalies in the North Pacific leading to reduced storm track activity through changes in the tropospheric baroclinicity [47]. Anomalously warm SSTs in the west-central Pacific also diverted storm tracks poleward [47]. However, other research has suggested that precipitation can be altered by dynamic atmospheric adjustments from perturbations in SSTs. Beaudin *et al* (2023) recently modeled the effects of extratropical Pacific SSTs with PDO-like patterns and found precipitation was altered through changes to water vapor fluxes driven towards California during the winter [40]. These water vapor fluxes were largely caused by changes to synoptic scale winds due to the atmospheric adjustments to SST anomalies in the NE Pacific [40]. Composites of SSTs and SLPs for high and low snow years suggests that the atmospheric adjustments are dynamic

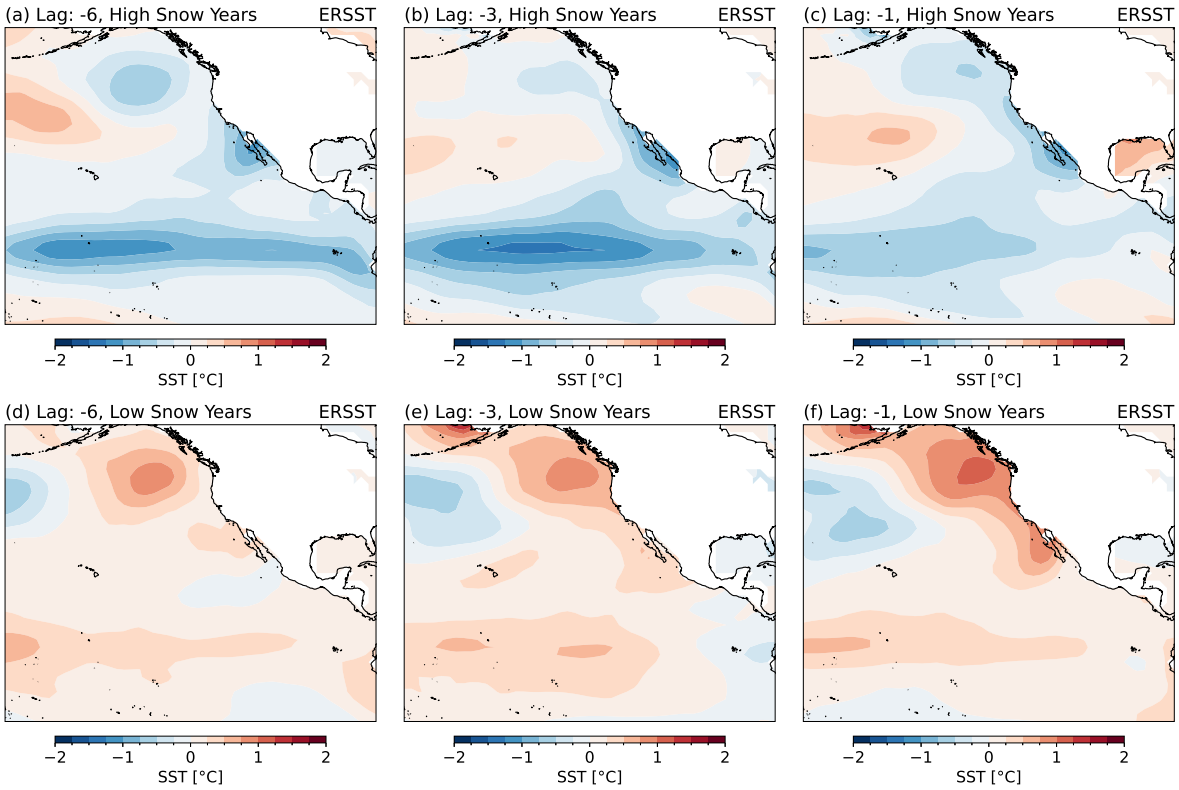

Figure 10. Similar to figure 9 but for SST anomalies.

rather than thermodynamic, since warm NE Pacific SSTs appear to favor low snow years anomalies.

4. Conclusions

We present one of the first applications of convergent cross mapping to snow prediction. Specifically, we use SSTs of the northeastern Pacific Ocean with nearly 60 years of snow measurements across the western United States and Canada. We have demonstrated that CCMs and causal statistics can provide useful information about snow dynamics in the Western United States and can potentially improve future projections of snowpack levels by including ocean temperatures off the coast for multiple ecoregions. We present convergent cross maps of SSTs of the central/eastern Pacific Ocean with nearly 60 years of snow measurements across the western United States and Canada. CCMs identified that NE Pacific SSTs can drive snowpack levels in the mountainous regions of the Pacific Northwest, like the Cascades Range, with lags of up to 6 months. Warm (cool) SSTs in the NE Pacific are associated with low (high) snow levels in the Pacific Northwest. The CCM results also suggests that the causal influence of SSTs and extratropical modes of climatic variability may play a larger role in changing winter snowpack levels compared to tropical modes such as ENSO. CCMs also seem to be sensitive to notable shifts in climate variability with increased predictability after 1999, likely due to the change from

the warm to cold phase of the PDO

CCM reconstructions of SWE from NE Pacific SSTs can predict high and low snow years with higher fidelity than lagged linear regression methods for the Pacific Northwest, especially at longer lags. CCMs may open the door for future SWE projections at longer timescales than is currently possible, allowing for efficient and effective water management solutions for the PNW. With projected increases in global ambient and ocean temperatures, considering ocean temperatures may be crucial in determining how to manage a diminishing snow water resources in this region. CCM may be a useful tool in the analysis of complex dynamical networks and helpful for generating hypothesis that be tested further via dynamical modeling.

Acknowledgments

The authors declare no conflicts of interest relevant to this study. We acknowledge the Information Technology and Services department at Syracuse University for its access and help to OrangeGrid (NSF award ACI-1341006). We also acknowledge Dr. Linda Ivany at Syracuse University for her feedback on very early versions of this manuscript. TB acknowledges support from NSF CAREER award OCE-2237502 and Sloan Foundation Fellowship FG-2023-20259. TB and DF acknowledge support from NSF P4Climate Award AGS-2402498.

Data availability

The data that support the findings of this study are openly available at the following DOI: https://doi.org/10.5281/zenodo.14918947.

References

[1] Hale K E, Jennings K S, Musselman K N, Livneh B and Molotch N P 2023 *Communications Earth & Environment* **4** 170 ISSN 2662-4435 URL https://www.nature.com/articles/s43247-023-00751-3

[2] Bales R C, Molotch N P, Painter T H, Dettinger M D, Rice R and Dozier J 2006 *Water Resources Research* **42** ISSN 00431397 URL http://doi.wiley.com/10.1029/2005WR004387

[3] Li D, Wrzesien M L, Durand M, Adam J and Lettenmaier D P 2017 *Geophysical Research Letters* **44** 6163–6172 ISSN 0094-8276, 1944-8007 URL https://agupubs.onlinelibrary.wiley.com/doi/10.1002/2017GL073551

[4] Mote P W, Li S, Lettenmaier D P, Xiao M and Engel R 2018 *npj Climate and Atmospheric Science* **1** 2 ISSN 2397-3722 URL https://www.nature.com/articles/s41612-018-0012-1

[5] Stewart I T, Cayan D R and Dettinger M D 2005 *Journal of Climate* **18** 1136–1155 ISSN 1520-0442, 0894-8755 URL http://journals.ametsoc.org/doi/10.1175/JCLI3321.1

[6] Roberts-Pierel B M, Raleigh M S and Kennedy R E 2024 *Water Resources Research* **60** e2023WR034588 ISSN 0043-1397, 1944-7973 URL https://agupubs.onlinelibrary.wiley.com/doi/10.1029/2023WR034588

[7] Sturm M, Goldstein M A and Parr C 2017 *Water Resources Research* **53** 3534–3544 ISSN 0043-1397, 1944-7973 URL https://onlinelibrary.wiley.com/doi/10.1002/2017WR020840

[8] Diffenbaugh N S, Swain D L and Touma D 2015 *Proceedings of the National Academy of Sciences* **112** 3931–3936 ISSN 0027-8424, 1091-6490 URL https://pnas.org/doi/full/10.1073/pnas.1422385112

[9] Reager J, Thomas A, Sproles E, Rodell M, Beaudoing H, Li B and Famiglietti J 2015 *Remote Sensing* **7** 14663–14679 ISSN 2072-4292 URL http://www.mdpi.com/2072-4292/7/11/14663

[10] Musselman K N, Lehner F, Ikeda K, Clark M P, Prein A F, Liu C, Barlage M and Rasmussen R 2018 *Nature Climate Change* **8** 808–812 ISSN 1758-678X, 1758-6798 URL https://www.nature.com/articles/s41558-018-0236-4

[11] Pomeroy J W, Fang X and Marks D G 2016 *Hydrological Processes* **30** 2899–2914 ISSN 08856087 URL https://onlinelibrary.wiley.com/doi/10.1002/hyp.10905

[12] Tsang L, Durand M, Derksen C, Barros A P, Kang D H, Lievens H, Marshall H P, Zhu J, Johnson J, King J, Lemmetyinen J, Sandells M, Rutter N, Siqueira P, Nolin A, Osmanoglu B, Vuyovich C, Kim E, Taylor D, Merkouriadi I, Brucker L, Navari M, Dumont M, Kelly R, Kim R S, Liao T H, Borah F and Xu X 2022 *The Cryosphere* **16** 3531–3573 ISSN 1994-0424 URL https://tc.copernicus.org/articles/16/3531/2022/

[13] Cayan D R 1996 *Journal of Climate* **9** 928–948 ISSN 0894-8755, 1520-0442 URL http://journals.ametsoc.org/doi/10.1175/1520-0442(1996)009<0928:ICVASI>2.0.CO;2

[14] Marshall A M, Abatzoglou J T, Rahimi S, Lettenmaier D P and Hall A 2024 *Proceedings of the National Academy of Sciences* **121** e2320600121 ISSN 0027-8424, 1091-6490 URL https://pnas.org/doi/10.1073/pnas.2320600121

[15] Harley G L, Maxwell R S, Black B A and Bekker M F 2020 *Climatic Change* **162** 127–143 ISSN 0165-0009, 1573-1480 URL https://link.springer.com/10.1007/s10584-020-02719-0

[16] Cayan D R, Redmond K T and Riddle L G 1999 *Journal of climate* **12** 2881–2893 iSBN: 0894-8755;1520-0442;

[17] Clark M P, Serreze M C and McCabe G J 2001 *Water Resources Research* **37** 741–757 ISSN 0043-1397, 1944-7973 URL https://agupubs.onlinelibrary.wiley.com/doi/10.1029/2000WR900305

[18] Pierce D W, Barnett T P, Hidalgo H G, Das T, Bonfils C, Santer B D, Bala G, Dettinger M D, Cayan D R, Mirin A, Wood A W and Nozawa T 2008 *Journal of Climate* **21** 6425–6444 ISSN 1520-0442, 0894-8755 URL http://journals.ametsoc.org/doi/10.1175/2008JCLI2405.1

[19] Seager R, Hoerling M, Schubert S, Wang H, Lyon B, Kumar A, Nakamura J and Henderson N 2015 *Journal of Climate* **28** 6997–7024 ISSN 0894-8755, 1520-0442 URL http://journals.ametsoc.org/doi/10.1175/JCLI-D-14-00860.1

[20] Seager R and Hoerling M 2014 *Journal of Climate* **27** 4581–4606 ISSN 0894-8755, 1520-0442 URL http://journals.ametsoc.org/doi/10.1175/JCLI-D-13-00329.1

[21] Wang S, Hipps L, Gillies R R and Yoon J 2014 *Geophysical Research Letters* **41** 3220–3226 ISSN 0094-8276, 1944-8007 URL https://onlinelibrary.wiley.com/doi/10.1002/2014GL059748

[22] Sugihara G, May R, Ye H, Hsieh C h, Deyle E, Fogarty M and Munch S 2012 *Science* **338** 496–500 ISSN 0036-8075, 1095-9203 URL https://www.science.org/doi/10.1126/science.1227079

[23] Musselman K N 2021 Daily snow water equivalent (SWE) observations from 1,065 stations in western North America for years 1960 - 2019. URL https://doi.org/10.5281/zenodo.4546865

[24] Dressler K A, Fassnacht S R and Bales R C 2006 *Journal of Hydrometeorology* **7** 705–712 ISSN 1525-7541, 1525-755X URL http://journals.ametsoc.org/doi/10.1175/JHM506.1

[25] Musselman K N, Addor N, Vano J A and Molotch N P 2021 *Nature Climate Change* **11** 418–424 ISSN 1758-678X, 1758-6798 URL https://www.nature.com/articles/s41558-021-01014-9

[26] Serreze M C, Clark M P, Armstrong R L, McGinnis D A and Pulwarty R S 1999 *Water Resources Research* **35** 2145–2160 ISSN 00431397 URL http://doi.wiley.com/10.1029/1999WR900090

[27] Trujillo E and Molotch N P 2014 *Water Resources Research* **50** 5611–5623 ISSN 0043-1397, 1944-7973 URL https://agupubs.onlinelibrary.wiley.com/doi/10.1002/2013WR014753

[28] Hunter T, Tootle G and Piechota T 2006 *Geophysical Research Letters* **33** 2006GL026600 ISSN 0094-8276, 1944-8007 URL

https://agupubs.onlinelibrary.wiley.com/doi/10.1029/2006GL026600

[29] Omernik J M and Griffith G E 2014 *Environmental Management* **54** 1249–1266 ISSN 0364-152X, 1432-1009 URL http://link.springer.com/10.1007/s00267-014-0364-1

[30] Huang B, Thorne P W, Banzon V F, Boyer T, Chepurin G, Lawrimore J H, Menne M J, Smith T M, Vose R S and Zhang H M 2017 *Journal of Climate* **30** 8179 – 8205 place: Boston MA, USA Publisher: American Meteorological Society URL https://journals.ametsoc.org/view/journals/clim/30/20/jcli-d-16-0836.1.xml

[31] Bonotto G, Peterson T J, Fowler K and Western A W 2022 *Water Resources Research* **58** e2021WR030231 ISSN 0043-1397, 1944-7973 URL https://agupubs.onlinelibrary.wiley.com/doi/10.1029/2021WR030231

[32] Runge J, Gerhardus A, Varando G, Eyring V and Camps-Valls G 2023 *Nature Reviews Earth & Environment* **4** 487–505 ISSN 2662-138X URL https://www.nature.com/articles/s43017-023-00431-y

[33] Wang Y, Yang J, Chen Y, De Maeyer P, Li Z and Duan W 2018 *Scientific Reports* **8** 12171 ISSN 2045-2322 URL https://www.nature.com/articles/s41598-018-30669-2

[34] Wazneh H, Gachon P, Laprise R, De Vernal A and Tremblay B 2021 *Climate Dynamics* **56** 2199–2221 ISSN 0930-7575, 1432-0894 URL https://link.springer.com/10.1007/s00382-020-05583-x

[35] Ye H and Sugihara G 2016 *Science* **353** 922–925 ISSN 0036-8075, 1095-9203 URL https://www.science.org/doi/10.1126/science.aag0863

[36] Cenci S and Saavedra S 2019 *Nature Ecology & Evolution* **3** 912–918 ISSN 2397-334X URL https://www.nature.com/articles/s41559-019-0879-1

[37] Stoelinga M T, Albright M D and Mass C F 2010 *Journal of Climate* **23** 2473–2491 ISSN 1520-0442, 0894-8755 URL http://journals.ametsoc.org/doi/10.1175/2009JCLI2911.1

[38] Sugihara G and May R M 1990 *Nature* **344** 734–741 ISSN 0028-0836, 1476-4687 URL https://www.nature.com/articles/344734a0

[39] Petchey O L 2016 Simplex projection walkthrough URL https://doi.org/10.5281/zenodo.57081

[40] Beaudin E, Di Lorenzo E, Miller A J, Seo H and Joh Y 2023 *Geophysical Research Letters* **50** ISSN 0094-8276, 1944-8007 URL https://onlinelibrary.wiley.com/doi/10.1029/2022GL102354

[41] Hu S, Zhang W, Watanabe M, Jiang F, Jin F F and Chen H C 2024 *Journal of Climate* **37** 3191–3204 ISSN 0894-8755, 1520-0442 URL https://journals.ametsoc.org/view/journals/clim/37/11/JCLI-D-23-0434.1.xml

[42] Ding R, Tseng Y, Di Lorenzo E, Shi L, Li J, Yu J Y, Wang C, Sun C, Luo J J, Ha K, Hu Z Z and Li F 2022 *Nature Communications* **13** 3871 ISSN 2041-1723 URL https://www.nature.com/articles/s41467-022-31516-9

[43] Baxter S and Nigam S 2015 *Journal of Climate* **28** 8109–8117 ISSN 0894-8755, 1520-0442 URL http://journals.ametsoc.org/doi/10.1175/JCLI-D-14-00726.1

[44] Zhao J, Kug J, Park J and An S 2020 *Geophysical Research Letters* **47** e2020GL088993 ISSN 0094-8276, 1944-8007 URL https://agupubs.onlinelibrary.wiley.com/doi/10.1029/2020GL088993

[45] Amaya D J 2019 *Current Climate Change Reports* **5** 296–307 ISSN 2198-6061 URL http://link.springer.com/10.1007/s40641-019-00142-x

[46] Nakamura M and Yamane S 2010 *Journal of Climate* **23** 6445–6467 ISSN 1520-0442, 0894-8755 URL http://journals.ametsoc.org/doi/10.1175/2010JCLI3017.1

[47] Gan B and Wu L 2013 *Journal of Climate* **26** 6123–6136 ISSN 0894-8755, 1520-0442 URL http://journals.ametsoc.org/doi/10.1175/JCLI-D-12-00724.1